DAMAGE AND CRACK GROWTH MODELLING BY FRACTURE PROCESS ZONE

V.N. Shlyannikov*

The strain energy density (SED) criterion is applied for analysing of the crack growth in full range of yielding. A fracture process zone (FPZ) local to the crack tip is defined and discussed in connection with the influence of the constraint effects in fracture.It can be estimated from the uniaxial mechanical properties of the material. Dimensionless constraint parameter is suggested depending on both the local elastic-plastic stress intensity and local fracture stress.According to SED- approach the above stresses are determined on the distance equal to the FPZ-size.The relation of connection between the constraint and damage parameters is suggested. It is shown that the damage parameter to describe satisfactory the well known mechanism of ductile - brittle transition for a mild steel at a temperature change taking into account the FPZ-size.Both experimental and analytical results are examined for subcritical crack growth under static loading that depends on the steel structures.

INTRODUCTION

In literature on the fracture mechanics the limitations of the single-parameter theory is discussed. One connects the observed fracture characteristic dependencies on cracked body geometry and its loading conditions with the influence of nonsingular term T at small-scale yielding and in the general case with the constraint parameter Q at full plastic fracture. Rice (1) have assumed that have to be correlation between nonsingular parameters T and S connected with the stresses σ_{xx} and σ_{zz} respectively lying in the normal planes. These stresses caused distinctions in the singular stress fields describing by the HRR-model and the numerical results based on the FEM and boundary layer formulation.O'Dowd and Shih(2,3) provided the theoretical basis to the distinctions observed in stress fields by introducing the additional parameter in HRR-model denoted as constraint parameter Q. In the subsequent works both quantitative and qualitative estimates for Q are presented. Anderson (4) suggested the damage function keeping within the range between the brittle and ductile fracture type and was given some generalization of two-parameter theory but did not determine the governing parameter γ connected with the fracture micromechanism.
The object of this work is modelling of the crack growth by FPZ and to analyse and describe the relation between constraint and damage parameters at fracture.

*Kazan Branch of the Moscow Energetical Institute, 420066, Kazan, Russia

Constraint Parameter

Let the uniaxial stress and strain relation of material is given by Ramberg-Osgood equation. If σ_f, ε_f denote the ultimate stress and ultimate strain, respectively, than the area under the true stress and true strain curve can be obtained as

$$\left(\frac{dW}{dV}\right)_c = \sigma_f \varepsilon_f - \int_0^{\sigma_f} \varepsilon \, d\sigma = \frac{\sigma_0^2}{E}\left[\frac{1}{2}\bar{\sigma}_f^2 + \frac{\alpha n}{n+1}\bar{\sigma}_f^{n+1}\right] \tag{1}$$

where α and n are strain hardening coefficients while E and σ_0 are respectively theYoung's modulus and yield strength of material.Note that $\bar{\sigma}_f = \sigma_f/\sigma_0$ and the critical value $(dW/dV)_c$ corresponds to failure of a material element as used in the strain energy density criterion.For a multiaxial state of stress, (dW/dV) can be expressed in terms of the normalized mean stress $\bar{\sigma}_m$ and effective or equivalent stress $\bar{\sigma}_e$ as

$$\left(\frac{dW}{dV}\right) = \int_0^{\varepsilon_{ij}} \sigma_{ij} d\varepsilon_{ij} = \frac{\sigma_0^2}{E}\left[\frac{1+\nu}{3}\sigma_e^2 + \frac{1-2\nu}{6}\sigma_m^2 + \frac{\alpha n}{n+1}\sigma_e^{n+1}\right] \tag{2}$$

with ν being the Poisson's ratio. Concept of the strain energy density by Sih (5) proceeds from an assumption that the critical SED value is reached on some distance from the crack tip r_c where the limiting transition conditions or equality of equations (1) and (2) are satisfied at fracture

$$\left(\frac{dW}{dV}\right)_C = \left(\frac{dW}{dV}\right)\Big|_{r=r_c} \tag{3}$$

Equation (2) may be performed to express the SED into σ_m/σ_e ratio and taking into account (1-3) can obtained following expression for the constraint parameter

$$D_{SH} = \left(\frac{\bar{\sigma}_e}{\bar{\sigma}_m}\right) = \left[\frac{(1-2\nu)\bar{\sigma}_e^2}{3\bar{\sigma}_f + \frac{6\alpha n}{n+1}\left(\bar{\sigma}_f^{n+1} - \bar{\sigma}_e^{n+1}\right) - 2(1+\nu)\bar{\sigma}_e^2}\right]^{1/2} \tag{4}$$

To take advantage of a equation (4) it is necessary to determine the singularity elastic-plastic stress intensity $\bar{\sigma}_e$ and local fracture stress $\bar{\sigma}_f$ as well.

Local fracture stress

Well known that the specimen thickness play a key role in characterisation of the three-dimensional crack-tip fields and constraint effect is dependent on distance to the tip and the free edge-surface of the specimen. Asusumed that the contour of plastic zone local to the crack tip have shape as it is shown in Fig.1 where t is thickness of cracked body and r_p^{2D} and r_p^{3D} plastic zone size on the free surface and mid-plane respectively. The coordinates of pionts (A and B) of transition from plane strain to plane stress are set by value $0.5r_p^{2D}/t$ which is connected to the width of the shear lips on a failured specimen surface. Results of many elasic-plastic finite element calculations confirmed that the normalized out-of-plane stress is had by distribution on thickness as it is shown in Fig.1 where $\bar{\sigma}_{yy} = \sigma_{yy}/\sigma_0$ is maximal stress near to the crack tip $\bar{\sigma}_{zz} = \sigma_{zz}/\sigma_0$ is out-of-plane stress.The change of $\bar{\sigma}_{zz}/\bar{\sigma}_{yy}$ ratio with thickness can be approximated by equation

$$\left(\frac{\bar{\sigma}_{zz}}{\bar{\sigma}_{yy}}\right)=\left(\frac{\bar{\sigma}_{zz}^{3D}}{\bar{\sigma}_{yy}}\right)\left(\frac{4h}{r_p^{2D}}\right)\sqrt{\left(1-\frac{z}{h}\right)\left(\frac{r_p^{2D}}{2h}+\frac{z}{h}-1\right)} \tag{5}$$

where $\bar{\sigma}_{zz}^{3D}/\bar{\sigma}_{yy}\approx 0.5\div 0.6$ for plane strain in a mid-plane. Let $\bar{\sigma}_f$ in eq.(4) makes sence local fracture stress along of crack front and in the mid-plane $\bar{\sigma}_u^{true}\approx\bar{\sigma}_f^{3D}$ where is the true ultimate tensile stress $\bar{\sigma}_u^{true}=\sigma_u/\sigma_0(1-\psi)$.For the purpose of the present analysis accepted the distribution on thickness of local fracture stress $\bar{\sigma}_f$ along crack front in a qualitative meaning repeats the behaviour of plastic zone size as it shown inFig.1.Then the distribution of the $\bar{\sigma}_f$ with thickness can be given by follwing equation

$$\sigma_f=\frac{\sigma_f^{3D}}{1-2\nu}\left[1-\frac{2\nu}{r_p^{2D}/4h}\sqrt{\left(1-\frac{z}{h}\right)\left[2\left(\frac{r_p^{2D}}{4h}\right)+\frac{z}{h}-1\right]}\right] \tag{6}$$

Singularity elastic-plastic stress intensity

According to the approach by Makhutov (6) for the strain hardening material the maximal elastic-plastic stress intensity $\bar{\sigma}_e^{\max}$ local to crack tip can be determined through appropriate stress concentration factor K_σ

$$\bar{\sigma}_e^{\max}=K_\sigma\bar{\sigma}_{yn}=\left(\bar{\sigma}_e^{el}\right)^{P_\sigma}\Big/\bar{\sigma}_{yn}^{\frac{1-T}{1+n}},\quad T=\bar{\sigma}_{yn}BY_{sp},\quad P_\sigma=\frac{2n-0.5(n-1)\left(1-\bar{\sigma}_{yn}\right)}{n(n+1)} \tag{7}$$

$$\sigma_e^{el}=\left\{\frac{\lambda^2}{2}+\frac{2\lambda T}{\sqrt{2}}+T^2-\left[\frac{\lambda^2}{2}++\frac{\lambda T}{\sqrt{2}}\right]\left(1+\frac{\sigma_{zz}}{\sigma_{yy}}\right)+\frac{\lambda^2}{2}\left[1-\frac{\sigma_{zz}}{\sigma_{yy}}+\left(\frac{\sigma_{zz}}{\sigma_{yy}}\right)^2\right]\right\}^{\frac{1}{2}};\quad \lambda=\frac{\bar{\sigma}_{yn}}{\sqrt{r/a}} \tag{8}$$

Here $\sigma_{yn}=\sigma_{yn}/\sigma_0$ is the nominal stress applied in the y-direction, $Y_{sp}(a/w)$ is the specimen geometry correction factor, B(a/w) is the inherent stress biaxiality ratio in various fracture specimen geometries, a is crack length, w is specimen width.At satisfaction of a condition (3), r/a in a eq.(8) makes sense the fracture process zone size.

Fracture process zone size

Determination of the FPZ will be made by application of the SED criterion. A critical distance r_c ahead of the crack tip is assumed to take place when the SED in an element may given by eq. (2) reaches certain critical value that can be measured from a uniaxial test as implied by eq.(1). A relative FPZ size $\bar{\delta}=r_c/a$ can than be introduced from eq.(3) taking into account eqs. (1) and (2)

$$\bar{\delta}_c=\left\{\frac{\bar{S}_2\pm\left[\bar{S}_2^2-4\left(\bar{W}_c^*-\bar{S}_3\right)\left(\bar{S}_1+\bar{S}_P\right)\right]^{1/2}}{2\left(\bar{W}_c^{'}-\bar{S}_3\right)}\right\}^2 \quad\text{where}\quad \bar{W}_c^*=\left(\frac{\sigma_0}{\sigma_{yn}}\right)^2\left[\frac{1}{2}\bar{\sigma}_f^2+\frac{\alpha n}{n+1}\bar{\sigma}_f^{n+1}\right] \tag{9}$$

Here $\bar{S}_i$ (i=1,2,3) and $\bar{S}_p$ are elastic and plastic SED factors respectively. The work by Shlyannikov (7) contain more details about determination of these factors. The local fracture stress $\bar{\sigma}_f$ is given by eq. (6).

Results and Discussion

Resulsts for two different type of specimens and steels will be examined and compared with the test data. Compact tension specimen (CTS) are made from 30Cr steel and used for tensile crack loading. Three different types of heat treatment are administered to the 30Cr steel resulting in the different microstructures referred to as steel A, B and C. The theoretical approach elaborated in present work was used to describe experiments by Ritchie et al (8) on the low-temperature fracture toughness of high-nitrogen mild (HNM) steel.The four point bending specimen (FPBS) are made from HNM and used for mode I crack extension.The formulae (9) were used to compute the FPZ-size δ. In Fig.2 is shownFPZ-size distributions with thickness of four-point-bending specimens. For the HNM steel in the temperature range of -145°C to -115°C r_c increased moderately exhibiting the lower shelf fracture toughness temperature dependence correspond to stress - controlled cleavage fracture micromechanism at plane strain and computed FPZ - size of approximate $\bar{\delta}_c$=0.0167 or $r_c = \bar{\delta}_c a$=200μm.A sharp change in FPZ size is observed as temperature changes from -115°C to -103°C which is indicative of a corresponding change in the local fracture micromechanism. The range from -95°C to -60°C correspond to the upper shelf where fracture runs by a strain - controlled ductile micromechanism and $\bar{\delta}_c$= 0.003 or $r_c = \bar{\delta}_c a$= 36μm. The compute results submitted on Fig.2 actually show position of a crack front at fracture for each given temperature. The static load-displacement curves are used to determine the nominal stress $\bar{\sigma}_n = \sigma_{yn}/\sigma_0$ Onset of crack growth corresponds to $\bar{\sigma}_{nc}$ and final fracture to $\bar{\sigma}_{n\max}$. Eq.(9) is used to compute the FDZ size δ for HNM and 30Cr steel. Plotted in Figs.3 and 4 inclusive are the values of K_1/K_{1C} versus δ/R_0 for HNM steel as temperature is changed and for 30Cr steel as structure types are varied. The size of plastic zone is R_0 in the crack growth direction when $\bar{\sigma}_n = \bar{\sigma}_{nc}$. Macrocrack initiation is assumed to occur when $\bar{\sigma}_n > \bar{\sigma}_{nc}$ and $K_1 > K_{1C}$. For the its increment, $\delta = \Delta a_i = \Sigma r_i$. Hence, $\delta/R_0 = \Delta a_i / R_0$ can be plotted such that the current crack length is $a_i = a_0 + \Delta a_i$. In Fig. 3 on the lower shelf from -145°C to -115°C FPZ is larger than R_0 and subcritical macrocrack growth does not occur. Within the transition region of -103°C to -90°C where R_0 << a, subcritical crack growth is also absent. At T=-75°C and -60°C as δ/R_0 <1 subcritical crack growth is took place. Note that in Fig.4 for the 30Cr steel type A δ/R_0 >1. That is FPZ size δ_c was larger than R_0 in the crack growth direction. In other words, the crack did not encounter any resistance in its way to form of the plastic zone. For the steel types B and C the FPZ are predicted to be inside the plastic zone and slow crack growth was made possible up to K_1/K_{1C}=1.2÷1.5.In the cases when δ/R_0 >1 for HNM and 30Cr steel,the FPZ becomes r_c being related to K_{1C} and $r_c = \bar{\delta}_c a$ can be regarded as a constant of a material.

Damage parameter

The values of FPZ -size by eq.(9) used for compute of constraint parameter D_{sh} is given by eq.(4) taking into account eqs. (5-8). Anderson(4) have proposed damage parameter ϕ. Let in our case $\gamma = D_{sh}$. Than D_{sh}=1 corresponds to stress controlled fracture.The

other limit, D_{sh} =0, is to strain-controlled failure and damage parameter is given by

$$\phi_{sh} = \left(\frac{\sigma_m}{\sigma_0}\right)^{D_{SH}} \bar{\varepsilon}_{pl}^{1-D_{SH}} \tag{10}$$

where σ_m is mean (hydrostatic) stress and ε_{pl} is the equivalent plastic strain. Figs.5 and 6 are plots of ϕ_{sh} values as function of $\overline{T}$ and D_{SH}. Presented the experimental results Ritchie(8) on Fig. 5 for the true ultimate tensile stress $\bar{\sigma}_u^{true}$ depending on tempetature of test in dimensionless coordinates so that $\overline{T} = T_{\min}/T$=1 for T=-145°C and $\overline{T}$ =2.5 for T=-60°C. Thus as constraint relaxes a bigger ϕ_{sh} is required to accumulate damage before failure for a strain-controlled mechanism. In return, a smaller ϕ_{sh} is required for fracture by cleavage mechanism as D_{SH} increases.Thus developed D_{SH}-ϕ_{sh} approach can be predict of constraint effect on a material's fracture resistance through FPZ.

REFERENCES

(1) J.R.Rice, *J.Mech.Phys. Solids,* Vol. 22, 1974,pp. 17-26.
(2) N.P.O'Dowd and C.F.Shih, *J.Mech.Phys. Solids,* Vol. 39, 1991, pp. 989-1015.
(3) N.P.O'Dowd and C.F.Shih, *J.Mech.Phys. Solids,* Vol. 40, 1992, pp.939-963.
(4) T.L.Anderson, "*Fracture Mechanics*", CRC Press, 1995.
(5) G.C.Sih, *Engng.Fract.Mech.,*Vol. 5, 1973, pp.365-377.
(6) N.A.Makhutov, "*Deformation Criteria of Fracture*",Mashinostroenie, Moscow, 1981.
(7) V.N.Shlyannikov, *Theoret.Appl.Fract.Mech.,* in published.
(8) R.O.Ritchie, J.F.Knott and J.R.Rice, *J.Mech.Phys. Solids,* Vol. 21, 1973, pp.395-410.

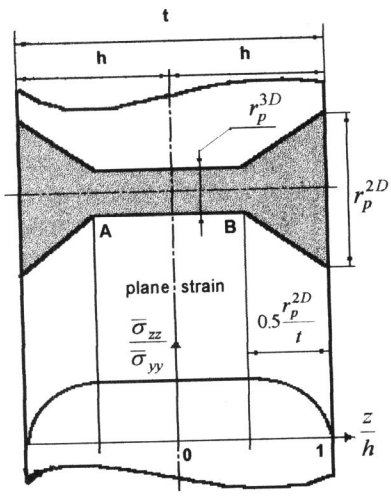

Figure 1 Schematic illustration of the constraint model

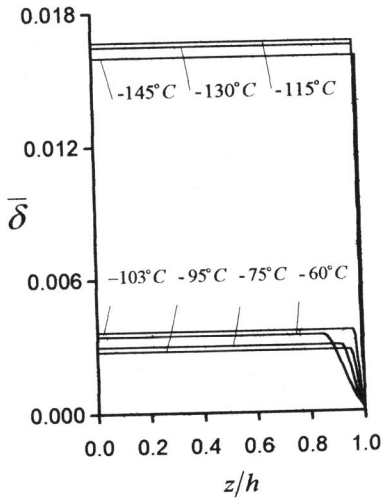

Figure 2 FPZ-size vs thickness for FPB-specimens of HNM steel

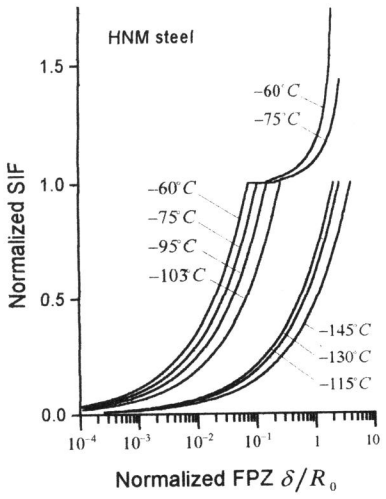

Figure 3 Crack growth curves of HNM with test temperature change

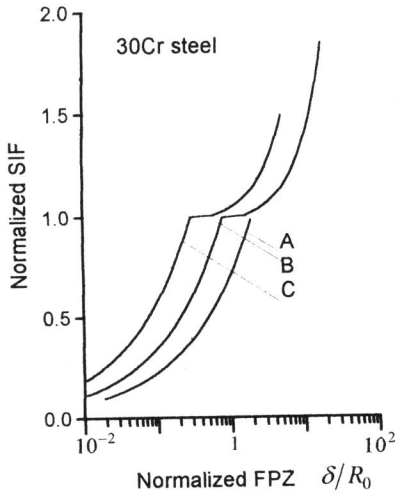

Figure 4 Crack growth curves of 30CR steel different structures

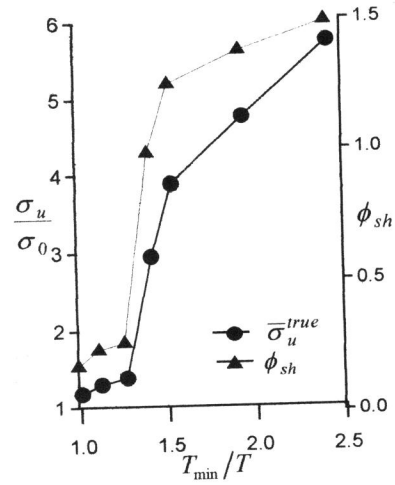

Figure 5 Strength and damage parameters vs test temperature

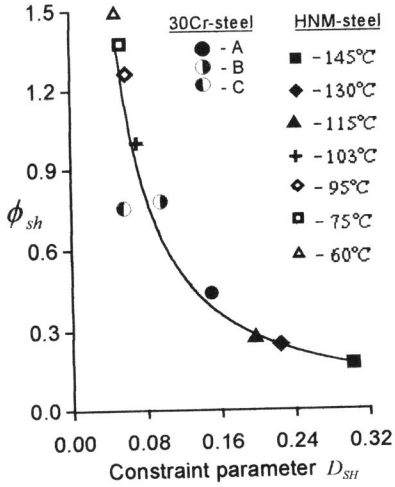

Figure 6 Dependence between damage and constraint parameters at fracture